A Wideband Coaxial-to-Ridge waveguide Adaptor

Kun Chen[1], Zhigang Wang[2], Dahai Ni[1], Hongbo Yin[1]
1.Yangzhou Haike Electronic Technology Corporation, Yangzhou, China.225000
2.University of Electronic Science and Technology of China, Chengdu, China.610000

Abstract: A Coaxial-to-ridge waveguide adaptor covering the entire K and Ka band has been demonstrated in this article. The adaptor is in the form of asymmetric double ridge waveguides and characteristic impedances of each step is determined by Chebyshev polynomial. A new method of calculating the characteristic impedance of the asymmetric double ridge waveguide is presented and the wideband adaptor is designed on this basis. The simulated results for the proposed adaptor in HFSS show that the return loss is better than 17.8dB in the entire K and Ka band and the insertion loss is better than 0.1dB. The simulated results for the back-to-back configuration show that return loss is better than 15 dB and insertion loss is better than 0.2dB. To demonstrate its performance, the adaptor is fabricated and then measured on the vector network analyser. The measured results show that the average insertion loss of the adaptor is about 1dB in the whole band.

Keywords: coaxial ridge waveguide adapter; Overlapping transformer steps; Chebyshev polynomial

1. INTRODUCTION

The rapid evolution of millimeter-wave technology has demonstrated tremendous application potential across fields including sensing and imaging, gesture recognition, short-range high speed data communication, mobile backhauls and last-mile connectivity1.Broadband, low-loss interconnects and components are critically important for future millimeter-wave applications2. Transmission lines in the form of rectangular or ridge waveguide are the first choice because their excellent performances on power capacity and low loss. In the past3-5, much attention has been paid to rectangular waveguide adaptor because of the flexibility it provides in system configurations. In comparison with rectangular ones, ridge waveguides have lower cut-off frequency, lower characteristic impedance and wider dominant mode bandwidth6. So the structures in the form of ridge waveguide are used more widely in implementing wideband lasers7-8.

In 20119, a wideband ridge waveguide to coaxial transition is designed and simulated in the form of symmetric double ridge waveguides and the VSWR is better than 1.3. In 10, a coaxial-to-quad-ridged circular waveguide transition is designed to feed the circular polarization quad-ridged waveguide circular horn and the simulated S_{11} is less than -10 dB. In 201611, a wideband coaxial to ridge gap waveguide transition is introduced with return loss better than 15 dB. The transition is designed of two successive parts and can be used with different ridge gap waveguide structures.

In this paper, an adaptor for coaxial waveguide to ridge waveguide has been demonstrated and fabricated. The transition parts are in the form of asymmetric double ridge waveguides. To the best of my knowledge, most of the work in the past are concentrated on symmetric double ridge waveguides until Mohamed A. Nasr and Ahmed A. KishK splitting the asymmetric double ridge waveguides into two single ridge waveguides from the electric wall. Since the boundary conditions remain unchanged, the field distributions in the two split single ridge waveguides are same with that in the double ridge waveguides. In their work, they give the position of the electric wall with the only asymmetric part being the ridge heights. On this basis, the characteristic impedance of the asymmetric double ridge waveguide is acquired from the characteristic impedance of the two split ridge waveguides by Mohamed A. Nasr and Ahmed A. Kishk.

In this paper, the derivation process of asymmetric double ridge waveguide with asymmetric part being both widths and heights of ridge is given in section 2. The design of the wideband adaptor from coaxial waveguide to ridge waveguide with asymmetric double ridge waveguides in the form of chebyshev is given in section 3. The test configurations and results are given in section 4.

2. ANALYSIS OF ASYMMETRIC DOUBLE RIDGE WAVEGUIDES

The geometry of the asymmetrical double ridge waveguide is shown in figure 1 with the asymmetric part being both the ridge heights and widths. The electric wall is right there to divide the asymmetrical double ridge waveguide into two parts with height b1 and b2. These two single ridge waveguide obviously have the same cut-off space with the original double ridge waveguide. One early calculation of the cut-off condition for symmetric single ridge waveguide is based on transverse resonance method. And the result can be applied to the split two parts to give

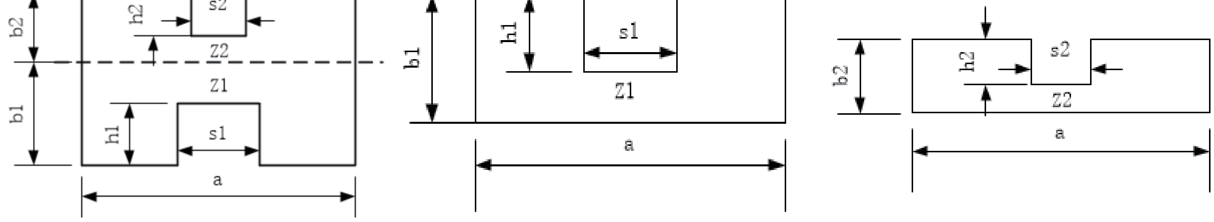

(a) (b) (c)

Figure 1 The asymmetrical double ridge waveguide. (a) Top view, (b) left-side view, and (c) right-sight view.

$$-\cot\theta_1 + \left(\frac{b_1}{d_1}\right)\tan(\theta_2) + 4\left(\frac{b_1}{\lambda_c}\right)\ln\left(\csc\left(\frac{\pi d_1}{2b_1}\right)\right) = 0 \quad (1)$$

$$-\cot\theta_3 + \left(\frac{b_2}{d_2}\right)\tan(\theta_4) + 4\left(\frac{b_2}{\lambda_c}\right)\ln\left(\csc\left(\frac{\pi d_2}{2b_2}\right)\right) = 0 \quad (2)$$

Where $\theta_1 = \frac{\pi(a-s_1)}{\lambda_c}$, $\theta_2 = \frac{\pi s_1}{\lambda_c}$, $\theta_3 = \frac{\pi(a-s_2)}{\lambda_c}$, $d_1 = b_1 - h_1$, $d_2 = b_2 - h_2$, $b_2 = b - b_1$, and $\theta_4 = \frac{\pi s_2}{\lambda_c}$.

When dealing with a specific double ridge waveguide, function (1) and function (2) can be boiled down to the system of nonlinear equations for variables b_1 and λ_c, which can be solved by some iterative methods. The values can sometimes be invalid and constraint conditions is $h_1 < b_1 < b - h_2$.

As a specific case, when $s_1 = s_2$, by making a subtraction between (1) and (2), the same conclusion can be drawn with that by Mohamed A. Nasr:

$$\frac{b_1}{d_1} = \frac{b_2}{d_2} \quad (3)$$

According to Mohamed A. Nasr's work, the impedance of the double ridge waveguide is given in terms of Z_{pv}. The expression is to some extent very complex and can be made some simplifications by assuming that the voltage is just in proportional to the distance in the middle of the ridge waveguide. As shown in figure 1, let the characteristic impedances of the two split ridge waveguide defined by power and voltage be Z1 and Z2 separately. So

$$Z1 = \frac{V_1^2}{2Pt_1} \quad (4)$$

$$Z2 = \frac{V_2^2}{2Pt_2} \quad (5)$$

$$\frac{V1}{V2} = \frac{d_1}{d_2} \quad (6)$$

V_1 and V_2 have the same phases as they are in the double ridge waveguide. The impedance of the double ridge waveguide can be deduced in the following way

$$Z = \frac{V^2}{2Pt} = \frac{(V_1+V_2)^2}{2(Pt_1+Pt_2)} \quad (7)$$

Taking (3) ,(4) and (5) into (6) with algebraic manipulations

$$Z = Z1 \times Z2 \times \frac{(\frac{d_1}{d_2}+1)^2}{Z2 \times (\frac{d_1}{d_2})^2 + Z1} \quad (8)$$

3. DESIGN METHOD FOR A WIDEBAND COAXIAL-TO-RIDGED ADAPTOR

The transition structure proposed in this paper has a 2.4mm Ka-type connector working up to 50 GHz chosen as input. The inner conductor of the coaxial connector expands to the hole on the low cavity steps which lies about a quarter waveguide wavelength from the short plane. The output ridge waveguide is 24JD18000 which can work spurious mode free until 44.3GHz, with a = 6.932mm, b = 3.119mm, s = 1.074mm, d = 1.300mm and the characteristic impedance in terms of power and voltage is about 193Ω. The transition steps are composed of 4 asymmetric double ridged waveguides with the initial values calculated by Chebyshev matching transformer. With the maximum reflection coefficient chosen to be 0.1, the impedances of the four steps are calculated to be 62.3Ω, 83.1Ω, 116.1Ω and 154.8Ω. The diagram shown in figure 2 shows the dimensions of the adaptor. Region 1, Region 2, Region 3 and Region 4 are asymmetric double ridge waveguides. W0 is set to be 2.31mm and H0 is determined by the formula in to make the characteristic impedance to be 50Ω. Then it comes to Region 1, this region as well as Region 2 to Region 4 are asymmetric double ridge waveguides with the only asymmetric parts being the ridge heights (although some asymmetric parts in ridge widths at the two ends). The dimensions of this steps are determined in the following way:

1.Set W1 to be 1.70mm and W2 to be 1.074mm which is the ridge width of 24JD18000. L1 = L11 = L2 = L21 = L3 = L31 = L4 = 2.6mm.

2.Then start form Region 4 with H41 being 1.819mm which is the ridge height of 24JD18000. With H4 being a variable ranging from 0~1.3mm, the characteristic impedance is calculated in Matlab by (3) and (8) to make it equal to 154.8Ω.

3.Then it turns to Region 3, making H3 and H31 being the variables and calculate the characteristic impedance to be 116.1Ω.

4.Region 2 and Region 1 are dealt with the same way as Region 3.

Finally, all the dimensions of W1, L1, L2, L3, L4, L11, L21, L31, H0, H1, H11, H2, H21, H3, H31 and H4 are optimized in full wave simulation platform to be W1 = 1.77mm, L1 = 0.92mm, L2 = 1.48mm, L3 = 1.11mm, L4 = 1mm, L11 = 1.21mm, L21 = 1mm, L31 = 1.09mm, H0 = 2.51mm, H1 = 2.05mm, H11 = 0.48mm, H2 = 1.38mm, H21 = 0.64mm, H3 = 0.46mm, H31 = 1.46mm and H4 = 0.2mm.

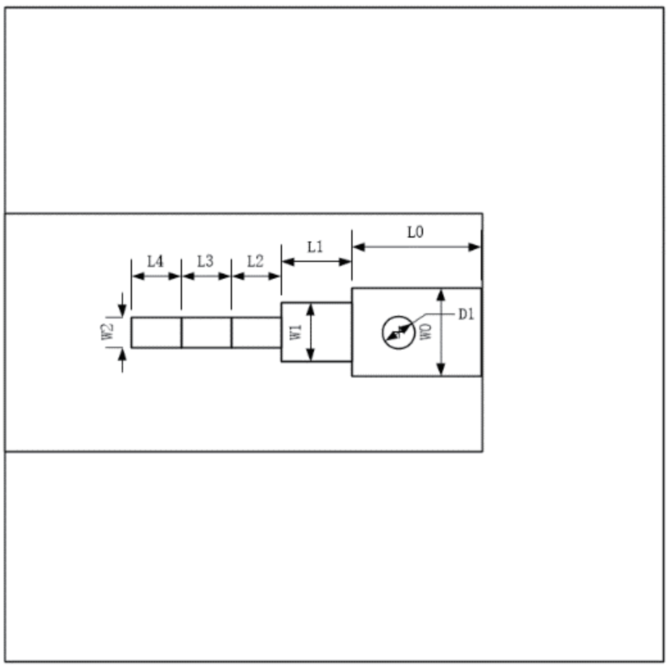

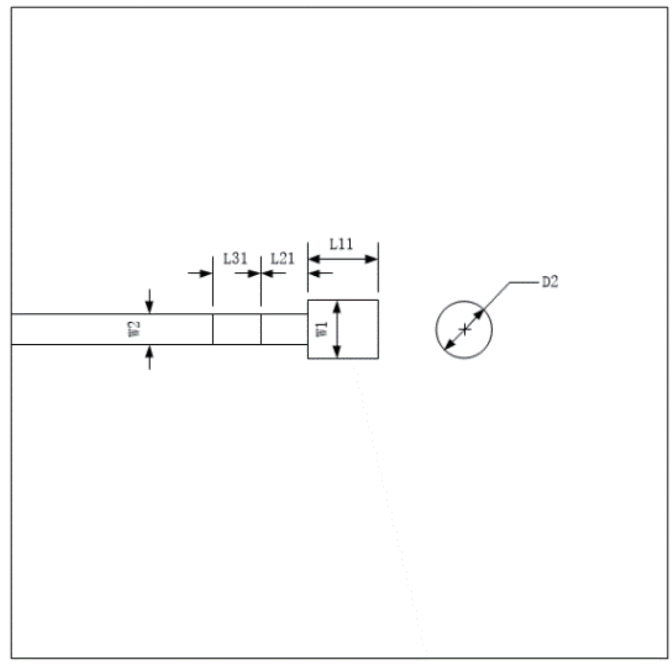

(a) The dimension of the upper steps. **(b) The dimension of the lower steps.**

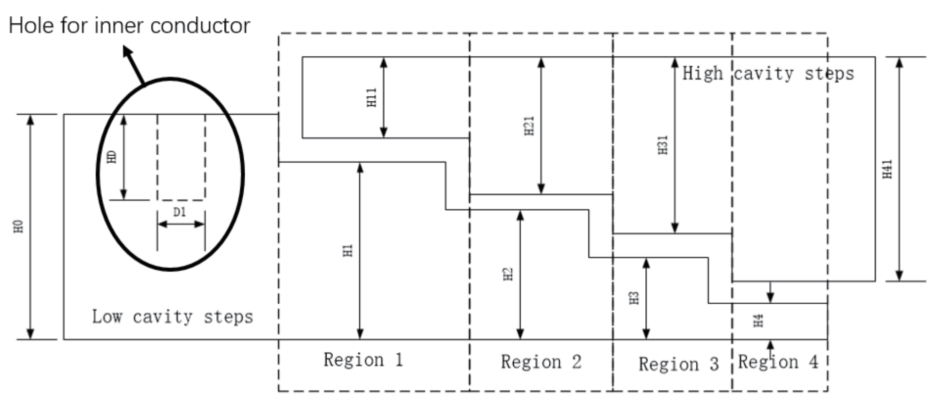

(c)Side view

Figure 2 The diagram of the coaxial-to-ridge waveguide adapter. (a) The upper steps, (b) the lower steps, and (c) the side view.

4. SIMULATION, FABRICATION , MEASUREMENT AND ANALYSIS

The simulated model in HFSS of the adaptor is shown in FIGURE 3 and the simulation results reveal the good performance of the adaptor with the return loss better than 17.8 dB over the whole band. Then, the cavity made of gold-plated aluminum is split from the upper face of the waveguide to become the low and up parts as shown in FIGURE 4. The test configuration is operated with two of the cavities and a 24JD18000 single ridge waveguide. The photograph of the test configuration and the simulation model is shown in FIGURE 4. The test results and the simulation results are drawn together in FIGURE 6 and they go well with each other.

(a)

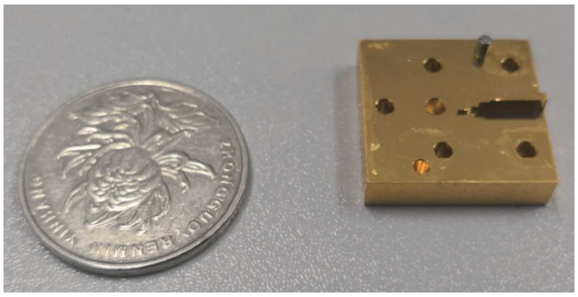

(b)

(c)

Figure 3 The coaxial-to-ridge waveguide adapter. (a) The upper cavity, (b) the lower cavity, and (c) the test configuration.

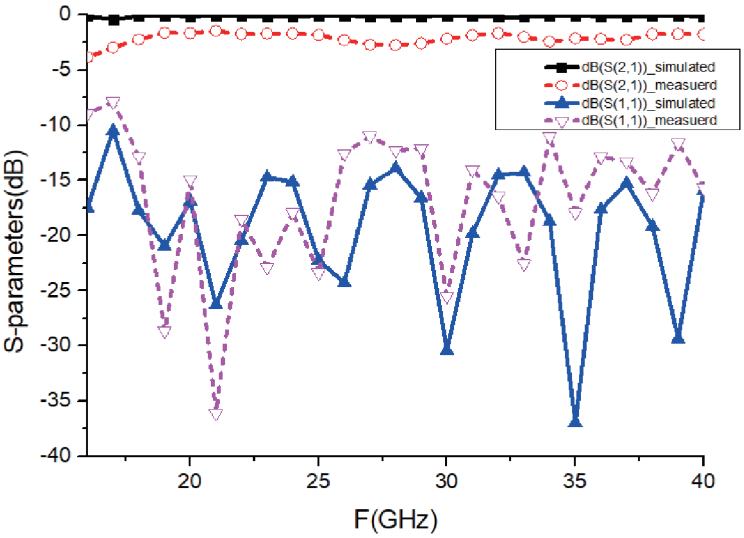

Figure 4 The simulated and measured results of the coaxial-to-ridge waveguide adapter.

5. CONCLUSION

A wideband coaxial-to-ridge waveguide adaptor covering the entire K and Ka band is analyzed and fabricated in this paper. The signal comes from the coaxial probe and runs in two ways with a part of it reflected back by the reflecting plane and added in phase with the other part. Then the recombined signal goes down through the well designed steps whose design process is introduced in detail. The simulation results reveal the success of the design method.

To validate the proposed topology, the adaptor is fabricated and measured on the vector network analyser. The measured results of the back-to-back configuration show that the average insertion loss is about 2 dB. So the insertion loss for the adaptor is about 1 dB in the whole band. The return loss is better than 11 dB in the whole band.

ACKNOWLEDGEMENTS

Hongzheng Sun has given very useful advice during the design process. Thanks a lot to his kindness.

REFERENCES:

[1] A. Niknejad and H. Hashemi. Mm-Wave Silicon Technology 60 GHz and Beyond [M]. New York, NY, USA: Springer, 2008.

[2]Nathan Jastram,Al-Tarifi, Ljubodrag Boskovic and Dejan S Filipovic. On the Split-Block Realization of Millimeter-Wave Ridge Waveguide Components [J]. IEEE Microwave & Wireless Components Letters, vol. 28, no. 4, April 2018.

[3] M. E. Bialkowski. Analysis of a coaxial-to-waveguide adaptor incorporating a dielectric coated probe [J]. IEEE Microwave & Guided Wave Lett, vol. I, no. 8, pp. 211-214, Aug. 1991.

[4] A. Ittipiboon and L. Shafal. Probe Mutual Impedance in a Rectangular Waveguide [J]. IEEE Transactions on Microwave Theory & Techniques, vol. MTT-33, no. 4, April 1985.

[5]A. Anger. Software compute Maxwell's equations [J]. Microwave J, vol. 33, no. 2, Feb. 1990.

[6] Ljubisa STANKOVIC and Svetozar JOVICEVIC. A round-ridge waveguide[J]. Ann. Telecommun 43, nos. 9-10, Oct. 1988.

[7]M. Wilkens. High-Efficiency Broad-Ridge Waveguide Lasers [J]. IEEE Photonics Technology Letters, vol. 30, no. 6, pp. 545-548, 15 March15, 2018.

[8]Wilkens. 970-nm ridge waveguide diode laser bars for high power DWBC systems [J]. High-power Diode Laser Technology, X VI 2018.

[9]Hopfer. The design of ridge waveguides. IRE Trans. Microwave Theory Tech [J], vol. MTT-3, pp. 20-29, October 1955.

[10]N. Marcuvitz. Waveguide Handbook[M], New York: McGraw Hill.ch.5. 1951.

[11] Lewin L. A contribution to the theory of probes in waveguides [J]. proc Inst Elec Eng,1958.

[12] Collin R E. Field Theory of Guide Waves[M], New York: McGraw-Hill, 1960, Ch.7:256-271.

[13]R. E. Collin. Field Theory of Guided Waves[M], New York: McGraw-Hill, Ch. 7. Math. Appendix, 1960.

[14]M. P. Pozar. Microwave Engineering[M], New York: John Wiley & Sons, Inc, 2012, ch. 5: 250-261.

KEYORDS: Coaxial-to-ridge waveguide adaptor, overlapping transformer steps, Chebyshev polynomial

About the author:

Kun Chen, (1982.8-), male, Han, born in Yangzhou, Jiangsu. He is a member of the Communist Party of China, a senior engineer, and holds a master's degree. He is engaged in microwave circuit design and serves as the Deputy General Manager of Yangzhou Haike Electronic Technology Co., Ltd. His